# THE TIKOKINO EARTHQUAKE OF 11 APRIL 1993: MOVEMENT AT THE PLATE INTERFACE IN SOUTHERN HAWKES BAY

**Martin Reyners[1,2], Peter McGinty[1], Jim Ansell[3,4] and Brian Ferris[1]**


## ABSTRACT

The nature of faulting that took place during the $M_L$ 5.9 Tikokino earthquake of 11 April 1993 has been determined using data from six temporary seismographs installed immediately after the event. The rupture initiated at 25 km depth, within the thrust zone between the subducted Pacific and overlying Australian plates. The earthquake had surprisingly few aftershocks, but those that did occur define a rupture zone which parallels the plate interface. When combined with the focal mechanism of the mainshock, this rupture zone indicates that the earthquake involved thrusting at the plate interface. The earthquake ruptured unilaterally to the south, and this explains the strong directivity seen in both strong motion accelerograph and seismograph records. Movement of the plate interface during the mainshock did not lead to significant triggering of other earthquakes in the subducted or overlying plates. A plausible explanation for the very few aftershocks is that the rupture initiated at an asperity at the plate interface and then propagated into subducted sediment lying in the conditionally stable frictional field. The nearby $M_L$ 6.1 Ashley Clinton earthquake of 1958, which also had a conspicuous absence of aftershocks, may have involved a similar process.


## INTRODUCTION

On 11 April 1993, a shallow $M_L$ 5.9 earthquake occurred near the small settlement of Tikokino in southern Hawkes Bay. It was felt widely in the southern part of the North Island (Fig. 1), and reported intensities reached MM7 at Waiiti station, 6 km northwest of Waipawa. Here unreinforced chimneys were brought down at the homestead, and movement of a grand piano during the earthquake punched a hole in a wall. Eight strong-motion records were retrieved following the earthquake (Cousins et al., 1994). The strongest recorded ground acceleration, 0.18g, was obtained from Waipawa, while 0.06g was recorded in Dannevirke, 0.03g in Hastings and 0.02-0.04g at three sites in Napier.

The earthquake occurred in a region where the velocity of the Pacific plate relative to the Australian plate is 42 mm/yr at an azimuth of 263° (DeMets et al., 1994). This relative motion is being accommodated by subduction of the Pacific plate and deformation of the overlying Australian plate. The subducted plate dips to the northwest, and the plate interface in the area of the Tikokino earthquake is about 20 km deep (Ansell and Bannister, 1996). The shock occurred near the southern end of the rupture zone of the $M_S$ 7.8 Hawkes Bay earthquake of 1931, an event which largely involved oblique thrusting within the overlying Australian plate (Haines and Darby, 1987). Moderately large shallow earthquakes have continued to occur in the region (Fig. 2), with those larger than $M_L$ 5.5 in the 40 years prior to the Tikokino event including the $M_L$ 6.1 Ashley Clinton earthquake of 1958, and an $M_L$ 5.6 earthquake in 1980. The latter event involved normal faulting in the uppermost part of the subducted plate (Reyners, 1983).

Immediately following the Tikokino earthquake, the Institute of Geological and Nuclear Sciences and Victoria University of Wellington installed six portable digital seismographs in the region, to supplement permanent stations of the National Seismograph Network (Fig. 2). The aim was to determine accurately the locations and mechanisms of aftershocks with this denser network, and hence determine the nature of the faulting that took place during the Tikokino event. The first portable station was installed 19 hours after the mainshock, and the portable network operated until 26 April. During that period 50 earthquakes of $M_L$ 1.6 - 4.4 were located in the region shown in Figure 2. This is a surprisingly small number of events following an $M_L$ 5.9 mainshock.


1 *Institute of Geological & Nuclear Sciences, Wellington*
2 *Member*
3 *Research School of Earth Sciences, Victoria University of Wellington*
4 *Deceased*

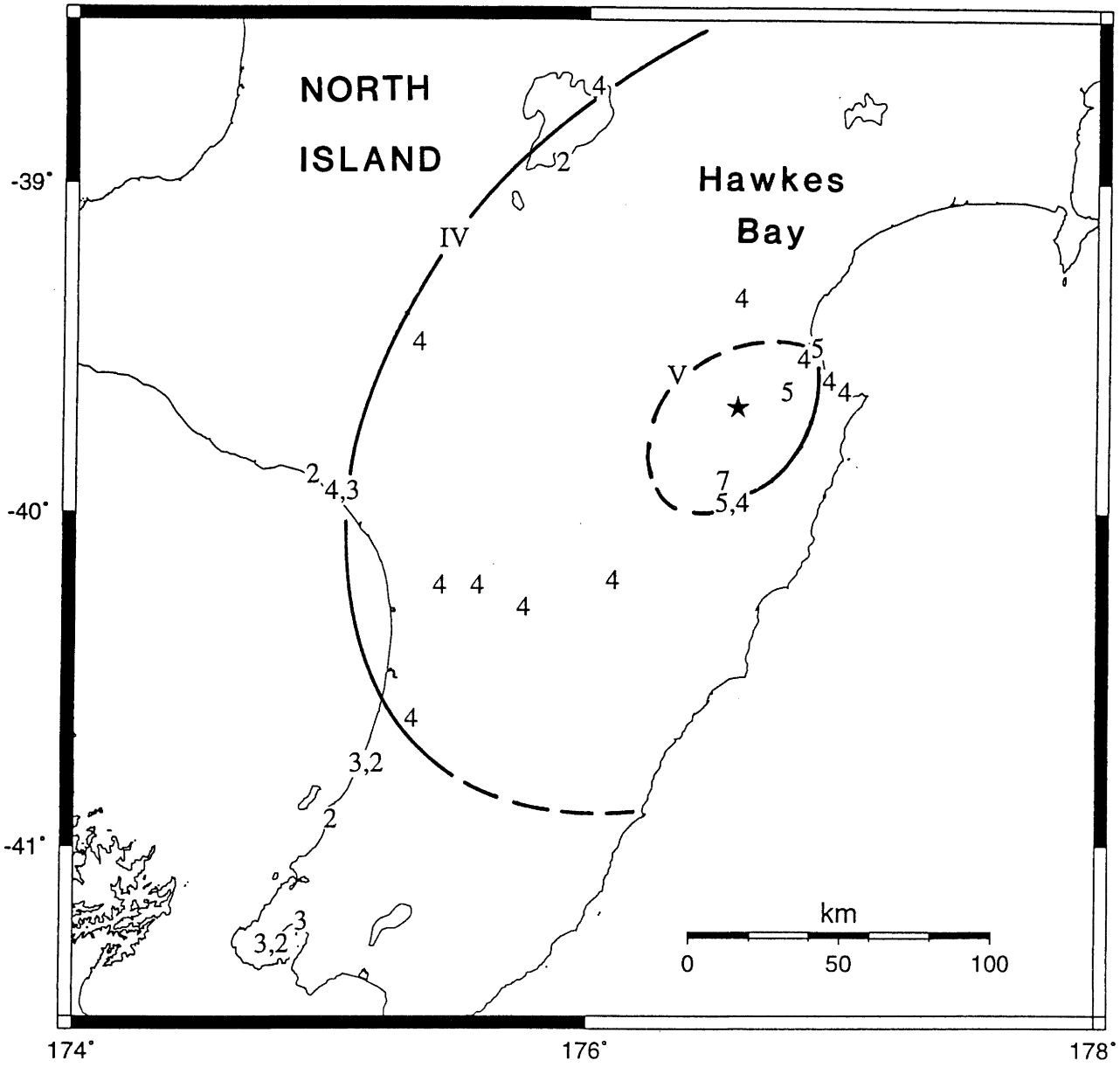


*FIGURE 1. Isoseismal map for the $M_L$ 5.9 Tikokino earthquake of 11 April 1993. Individual observations are indicated by a numeral giving the modified Mercalli intensity, and the star denotes the epicentre of the mainshock as relocated in this study.*

## RELOCATION OF EARTHQUAKE SEQUENCE

Data from the portable seismograph network provide the opportunity to improve on routinely determined earthquake locations, which use standard velocity models without station corrections. The relative paucity of events, combined with their uneven depth distribution (all but two were routinely located deeper than 20 km), precludes the determination of a new seismic velocity model of the region through the inversion of earthquake arrival times. To relocate the earthquake sequence, the seismic velocity model determined by Robinson (1994) for the Weber region, some 75 km to the southwest along the strike of the subducted plate, was adopted (Table 1). The two uppermost crustal layers and the upper mantle layer of this model have been fixed to those found in a crustal refraction experiment along the east coast of the North Island, which passed through the southeastern corner of the study area (Chadwick, 1997). The depth to the plate interface in the model was fixed at 20 km, that estimated by Ansell and Bannister (1996) for the centre of the study region. A Wadati plot indicates an average P-wave to S-wave velocity ratio of 1.69, and this was used for all layers in the seismic velocity model.

An inversion for both hypocentres and station corrections was performed using this velocity model. During the inversion, the portable station OHUT was used as a reference station, and its P-wave station correction was fixed at zero. The resulting

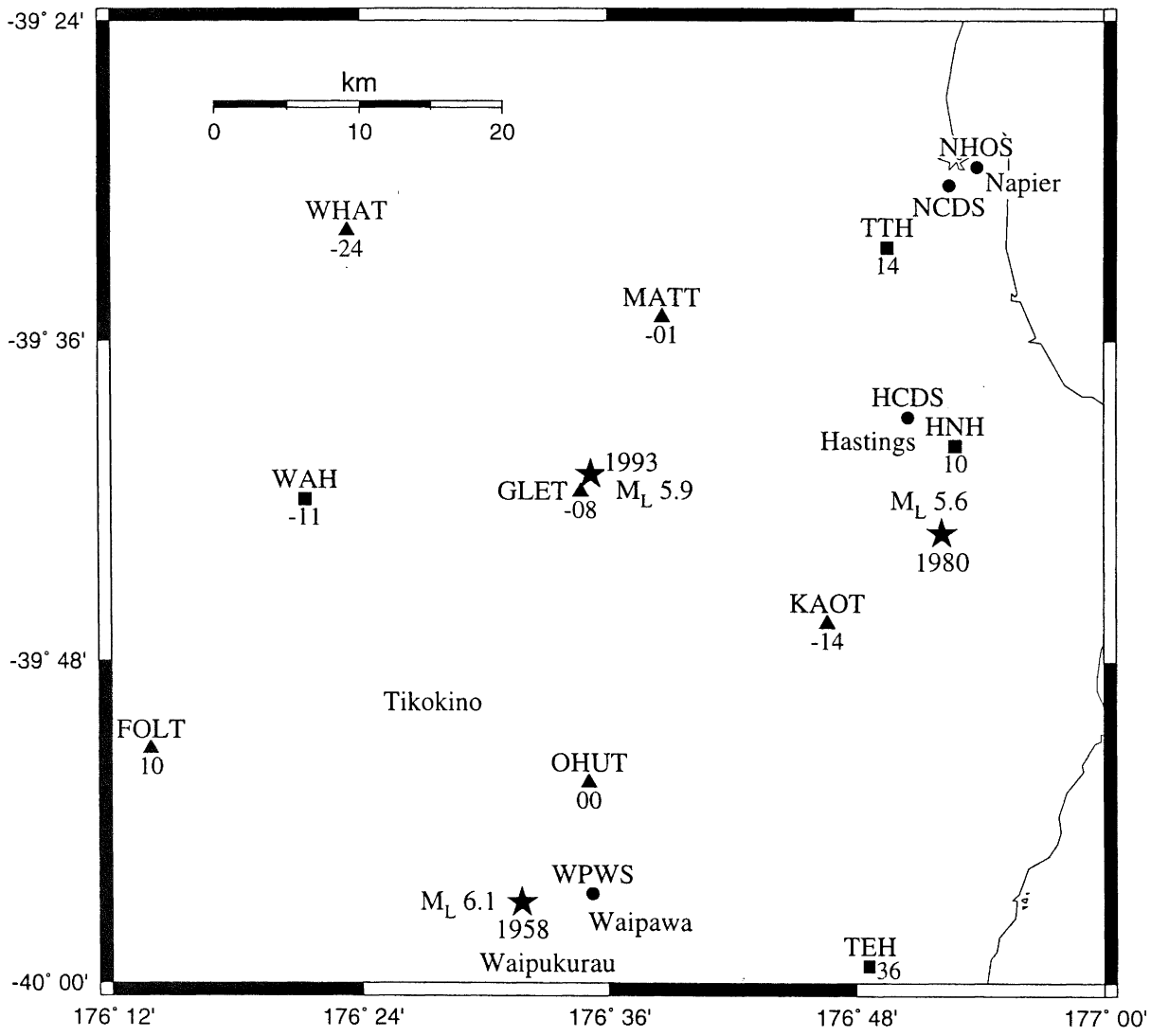


*FIGURE 2. The southern Hawkes Bay region. The Tikokino earthquake (as relocated in this study) is shown by a star, as are previous shallow events with $M_L$ > 5.5 in 1958 and 1980. Squares are permanent stations of the National Seismograph Network, circles are permanent strong motion accelerographs, and triangles are portable three-component seismographs installed immediately after the Tikokino earthquake. Station corrections for P-waves (in hundredths of a second) relative to station OHUT are shown next to each seismograph station.*

pattern of station corrections is shown in Figure 2. Although the mapping of a real, complex 3-D seismic velocity structure into a 1-D model as has been done here makes detailed interpretation unwise, the station corrections are broadly consistent with surface geology. They generally increase from the greywacke ranges in the northwest to the coast, reflecting a thickening of low-velocity sediments in this direction.

The station corrections were then used to relocate the whole earthquake sequence, from April 11-26. The resulting hypocentres are shown in Figure 3, graded by location quality using the criteria listed in Table 2. The mainshock is relocated at 25.4 ± 0.8 km depth, in contrast to the 34.5 ± 3.1 km determined during routine processing. The relocated epicentre is 39.68°S 176.59°E, 10 km WNW of the routinely determined epicentre (39.72°S 176.70°E). This new hypocentre is

**TABLE 1 Seismic Velocity Model**

| Layer | Depth (km) | Vp (km/s) |
|---|---|---|
| 1 | 0.0 - 4.0 | 3.55 |
| 2 | 4.0 - 8.0 | 5.35 |
| 3 | 8.0 - 13.0 | 5.94 |
| 4 | 13.0 - 20.0 | 6.29 |
| 5 | 20.0 - 25.0 | 6.10 |
| 6 | 25.0 - 35.0 | 7.49 |
| 7 | >35.0 | 8.77 |

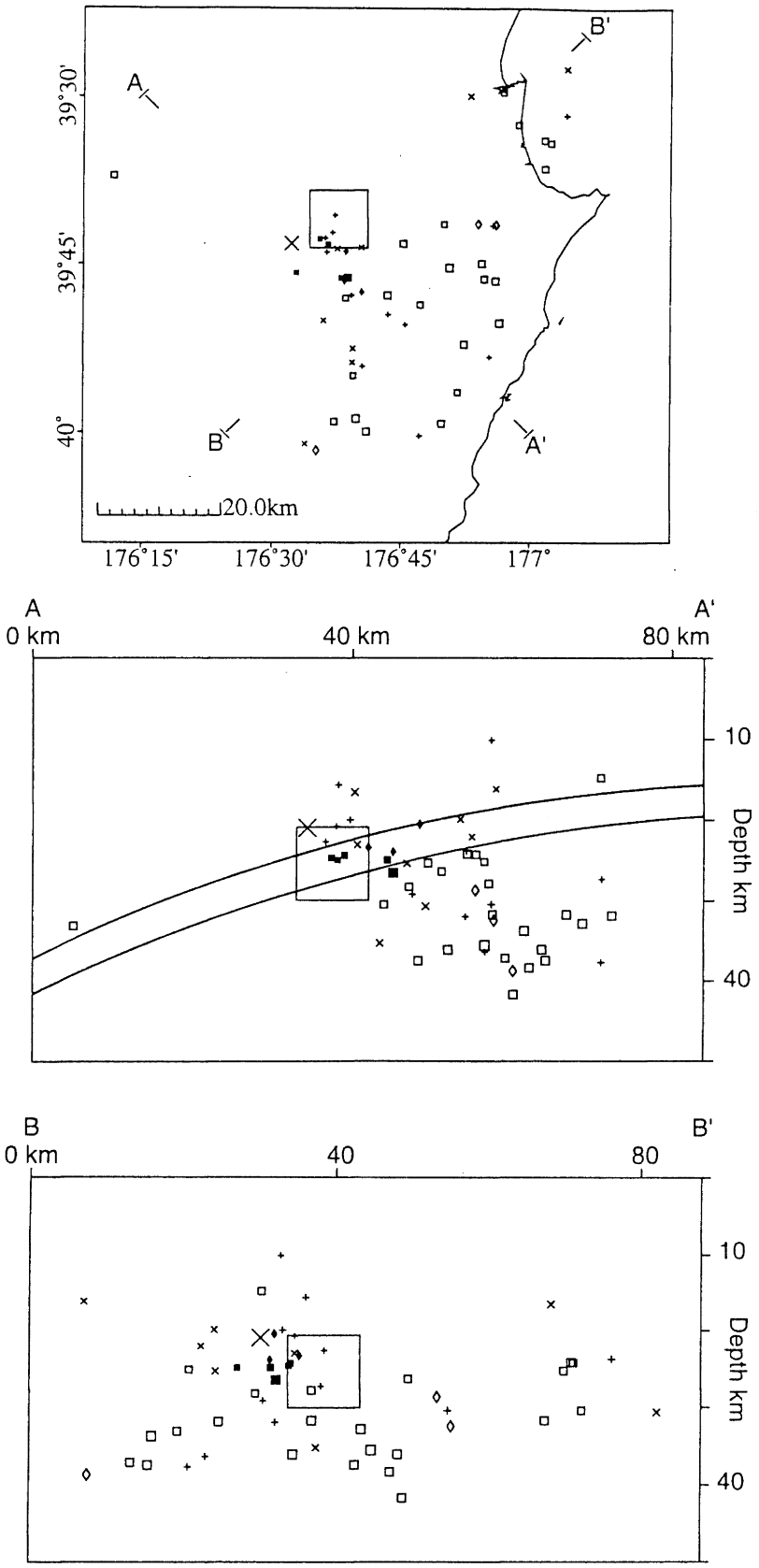


*FIGURE 3. Relocated earthquakes for the period 1993 April 11-26. Depth sections AA′ and BB′ are oriented down the dip and along the strike of the subducted Pacific plate, respectively. Hypocentres are scaled to magnitude and keyed to location quality (squares for A quality, diamonds for B, crosses for C and pluses for D; see Table 2). The large square is the mainshock hypocentre. A and B quality hypocentres interpreted as aftershocks are shown as filled symbols. The double line in section AA′ shows the interplate thrust zone defined by Ansell and Bannister (1996).*

**TABLE 2 Location quality criteria**

| Quality | A | B | C | D |
|---|---|---|---|---|
| Distance to Nearest Station, km | ≤1.5*Depth | ≤2*Depth | ≤3*Depth | >3*Depth |
| Number of Stations | ≥6 | ≥5 | ≥4 | 3 |
| RMS Travel-Time Residual, sec | ≤0.15 | ≤0.20 | ≤0.35 | ≤0.50 |
| Number of Phases | ≥8 | ≥6 | ≥5 | ≥4 |
| Convergence | Yes | Yes | Yes | Yes |
| S.E. of X and Y, km | ≤1.0 | ≤2.0 | ≤3.0 | >3.0 |
| S.E. of Depth, km | ≤1.0 | ≤2.0 | ≤3.0 | >3.0 |
| S.E. of Origin Time, sec | ≤0.10 | ≤0.15 | ≤0.20 | >0.20 |
| At Least One S Phase | Yes | Yes | Yes | Yes |

S.E. denotes standard error

consistent with the S minus trigger times recorded at the strong motion accelerographs at Waipawa, Hastings and Napier (Cousins et al., 1994). When these times are added the location of the mainshock is essentially unchanged. The new depth is also consistent with the 26 ± 2 km obtained from body-wave modelling of the mainshock (Webb and Anderson, 1997).

## FOCAL MECHANISMS

Even though installation of the portable seismographs achieved a station spacing of about 20 km, it is still generally not possible to usefully constrain the focal mechanisms of individual earthquakes in the sequence using P-wave first motion polarities alone. Thus we have supplemented the first motion polarities with data on the amplitudes of seismogram envelopes, which we compare with the envelopes of complete theoretical seismograms. The method is discussed in detail by Robinson and Webb (1996). The focal mechanism program places primary importance on the first motion data, and uses the amplitude data only to improve the resolution or remove ambiguities.

Using this technique, focal mechanisms were determined for all twenty earthquakes of $M_L \geq 2.3$. These are shown in map view in Figure 4, together with the mechanism for the mainshock determined by Webb and Anderson (1997) from body-wave modelling of teleseismic waveforms. Projections of the principal axes of compressional (*P*) and tensional (*T*) strain of the mechanisms are shown in Figure 5.

## DISCUSSION

### *Aftershock zone and rupture directivity*

Relocation of the mainshock places it within the interplate thrust zone defined by Ansell and Bannister (1996) [see Fig. 3]. This low velocity zone was found by Bannister (1988) to have a P-wave velocity between 3.0 - 4.7 km/s in Hawkes Bay, the exact velocity depending on the layer thickness. A similar low velocity zone near the plate interface has been found in the Weber region by Robinson (1994). This corresponds to the velocity inversion between 20 and 25 km in the model used to relocate earthquakes in this study (Table 1). The nature and thickness of the interplate thrust zone may be expected to vary along strike and down the dip of the subduction zone. Physically, it may represent a crush zone together with subducted sediments and volcanic knolls, as are seen offshore at the onset of subduction (e.g. Collot et al., 1996).

The paucity of aftershocks makes identification of the aftershock zone difficult. Also, as many of the aftershocks occurred before the installation of the portable seismographs, their relocated hypocentres have large errors, particularly in depth. We have inferred an approximate aftershock zone by considering only better quality (A and B) hypocentres which are close to the mainshock. Aftershocks identified in this way are shown as filled symbols in Figure 3. The inferred aftershock zone extends about 12 km south of the mainshock, and appears to parallel the interplate thrust zone. When depth errors are considered, many of the nearby C and D quality events, including the $M_L$ 4.4 event two days after the mainshock, could also have occurred within this aftershock zone.

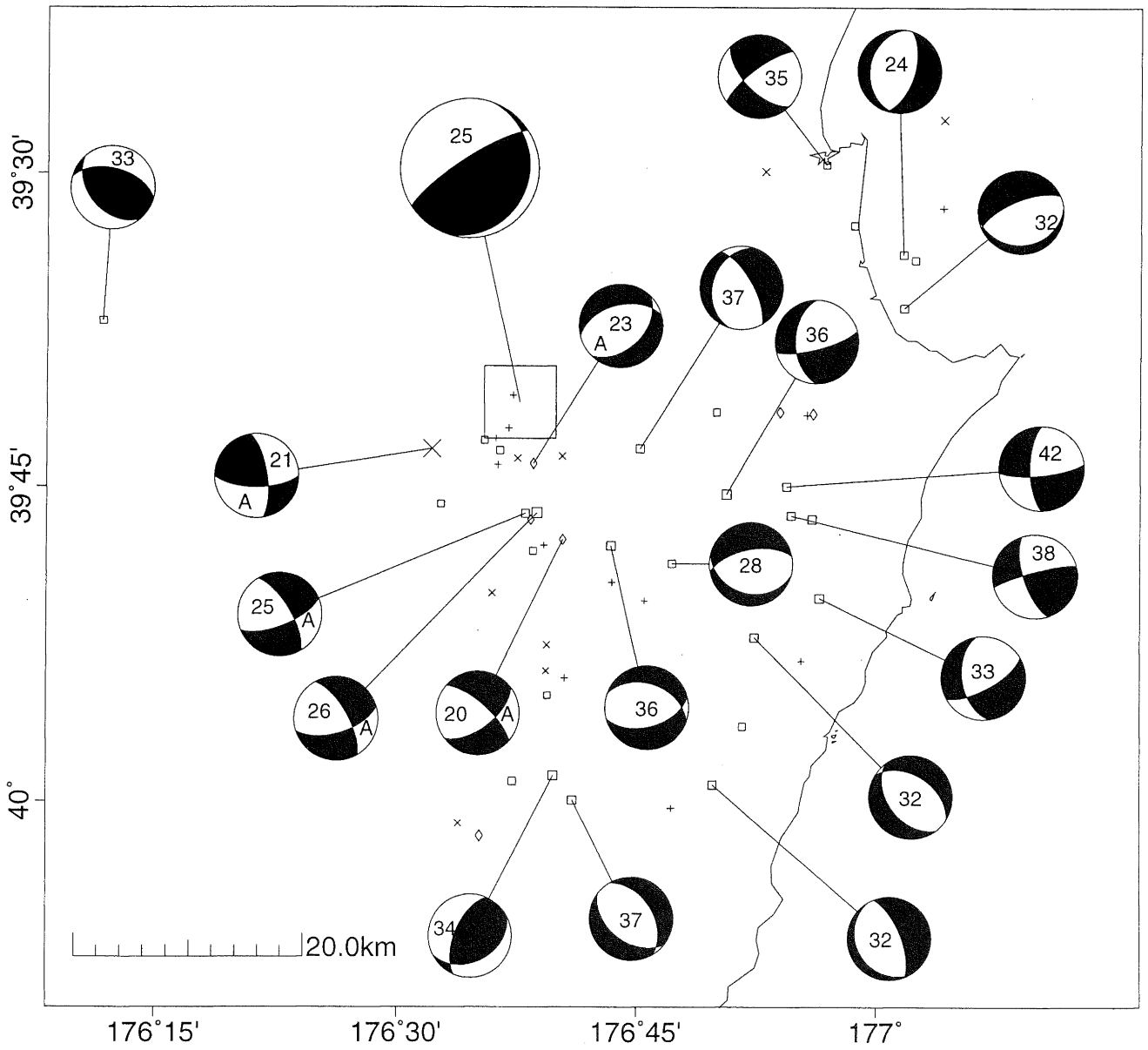


***FIGURE 4.*** ***Focal mechanisms of all earthquakes of $M_L \geq 2.3$. The mechanisms are equal area projections of the upper focal hemisphere, with compressional quadrants shaded. Numbers indicate earthquake depth in km. The larger mechanism is the mainshock, and aftershock mechanisms are labelled with the letter A.***

The aftershock zone gives an indication of the fault which ruptured during the mainshock. However, when it is defined from two weeks of aftershocks, as is the case here, it is likely to provide an upper limit on the fault area, since aftershock areas often expand with time after the mainshock (e.g. Tajima and Kanamori, 1985). The location of the mainshock hypocentre in relation to the aftershock zone suggests that the earthquake involved unilateral rupture to the south. Herein lies an explanation for the strong directivity seen in strong motion (Cousins et al., 1994). Peak ground acceleration at the nearest strong motion accelerograph (Hastings Civil Defence Headquarters, 23 km east of the mainshock epicentre) was only 0.03g, while the peak ground acceleration at Waipawa Post Office (29 km to the south of the epicentre in the direction of rupture) was 0.18g. This disparity in peak ground acceleration is unlikely to be caused by site effects alone. Indeed, relative amplification of ground motion might have been expected at Hastings rather than Waipawa, given that the depth to bedrock at Hastings is about 1000 m, while at Waipawa it is only 10 m. Significant reverberation is seen in the Hastings strong motion record, suggesting a site effect, while that from Waipawa is relatively clean (Cousins et al., 1994). Preliminary modelling of the strong motion data with a finite fault model confirms that the disparity in strong motion can be satisfactorily explained by rupture to the south on a fault some 7 km long and 2 km wide (R. Abercrombie and R. Benites, pers. comm., 1997).

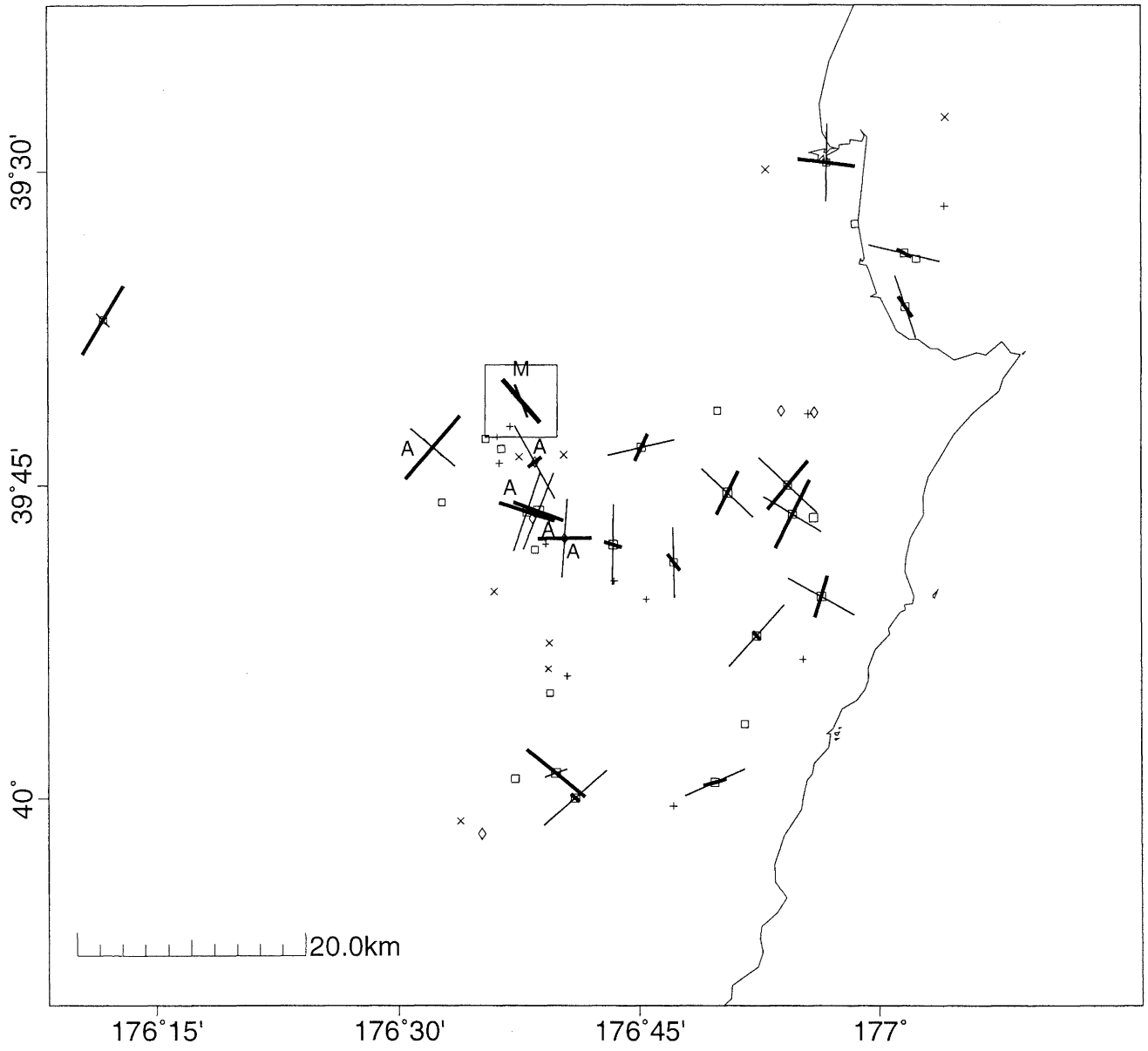


*FIGURE 5. Projections of the P-axes (heavy bars) and T-axes (light bars) of the focal mechanisms shown in Fig. 4. The mainshock and aftershocks are denoted by M and A, respectively.*

Directivity is also evident in seismograms recorded by the National Seismograph Network (Figure 6). Stations to the north of the earthquake recorded systematically lower seismic wave amplitudes (and hence magnitudes) than those to the south. This is unlikely to be due to path or site effects, given that a similar distribution of magnitudes is not seen for the nearby Weber earthquakes of 19 February 1990 ($M_L$ 6.1; located in the upper part of the subducted plate) and 13 May 1990 ($M_L$ 6.2; in the overlying plate). The magnitudes shown in Figure 6 have been calculated using the relocated hypocentre for the Tikokino earthquake. The average magnitude is $M_L$ 5.9, more in line with the $M_W$ 5.6 determined by Webb and Anderson (1997) from body-wave modelling than the $M_L$ 6.1 determined using the deeper, routinely determined hypocentre.

The intensity data shown in Figure 1 are insufficient to demonstrate large-scale directivity effects. However, it is noteworthy that the highest recorded intensity was south of the hypocentre, in the inferred direction of rupture.

### *Tectonic significance*

The orientation of the aftershock zone suggests that the shallowly-dipping nodal plane of the focal mechanism of the mainshock (Fig. 4) is the fault plane. As this fault plane parallels the plate interface, the Tikokino earthquake can be interpreted as an interplate thrust event. The five aftershocks for which mechanisms have been determined (labelled A in Figs. 4 and 5) show a variety of mechanisms. None replicate the thrusting at the plate interface which took place during the

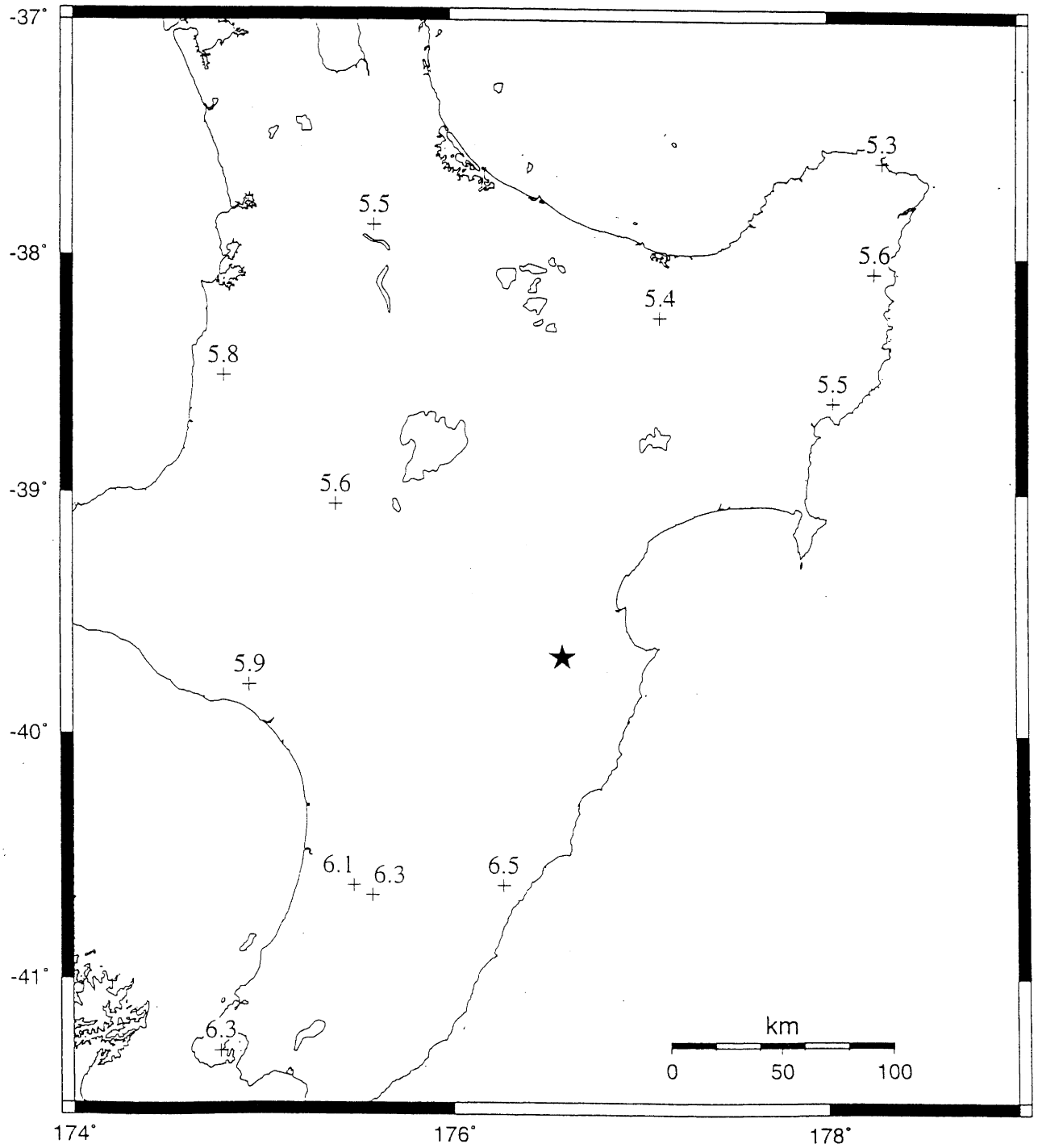


***FIGURE 6.*** ***Determinations of $M_L$ at individual stations of the National Seismograph Network (crosses) for the Tikokino earthquake (star).***

mainshock. On the other hand, focal mechanisms for events within the subducted plate reveal a more consistent pattern. Northeast of a line down the dip of the subducted plate through the mainshock epicentre, *T*-axes are generally subhorizontal and oriented in the direction of dip of the plate (Fig. 5). However, southwest of this line, where the mainshock rupture occurred, *T*-axes are generally subhorizontal and oriented along the strike of the subducted plate. A plausible explanation of this pattern is that the thrusting at the plate interface during the mainshock has relieved some of the pull from the deeper part of the subducted plate, leading to a rotation of *T*-axes out of the down-dip direction in the southwest. Alternatively, the pattern may be a long-term feature related to variation in plate coupling along the strike of the subduction zone. Such an interpretation is suggested by its location at the southern end of the rupture zone of the $M_S$ 7.8 Hawke's Bay earthquake of 1931, and the continuing occurrence of moderately large earthquakes in the area (Fig. 2). The 1980 earthquake in the subducted plate had a *T*-axis oriented down the dip of the subducted plate (Reyners, 1983), similar to those of nearby earthquakes in this study.

With the exception of the aftershock zone, the distribution of seismicity shown in Figure 3 is typical of that seen previously in the area, with the great majority of earthquakes occurring in the subducted plate, and very few in the overlying plate (e.g. Chong, 1982). Since the completion of the upgrade of the National Seismograph Network to digital recording in 1990, coverage of the area has been complete down to $M_L$ 2.9. Based on the average occurrence of such events since 1990, we would have expected a background seismicity rate of about three events of $M_L \geq 2.9$ during the period of this study. Excluding aftershocks, seven such events occurred. This is higher than average, but not unusually so. Seven or more earthquakes have occurred in the area in a similar 15-day period six times since 1990, without the occurrence of a large earthquake. Thus movement at the plate interface during the mainshock has not led to significant triggering of other earthquakes in the subducted or overlying plates.

A recent compilation of aftershock sequence parameters for shallow New Zealand earthquakes (D. Eberhart-Phillips, pers. comm., 1997) suggests that on average one would expect about 100 aftershocks of magnitude 2.9 or more in the first two weeks following an $M_W$ 5.6 mainshock. Thus the aftershock sequence of the Tikokino earthquake is rather anomalous, given that only two such aftershocks occurred. A lack of aftershocks in the zone where a large amount of slip occurred at the plate interface during the $M_W$ 7.7 1992 Nicaragua earthquake has been attributed to sediments at the plate interface lying in the conditionally stable frictional field (Ihmlé, 1996). The possible frictional stability states for subducted sediment have been discussed by Scholz (1990, p. 320). In the conditionally stable field, slip normally occurs aseismically, but seismic slip can occur if triggered by slip in a neighbouring unstable region. Given the likelihood of subducted sediment in the region of the Tikokino earthquake (Bannister, 1988), a similar explanation for the lack of aftershocks is tenable. The Tikokino earthquake may have initiated at an asperity (rough spot) at the plate interface lying in the unstable frictional field. Rupture may then have propagated into subducted sediment lying in the conditionally stable field.

It is noteworthy that the Tikokino earthquake was similar in many respects to the $M_L$ 6.1 Ashley Clinton earthquake of 1958. This event occurred some 30 km south of the Tikokino event (Fig. 2). It also had a conspicuous absence of identifiable aftershocks (New Zealand Seismological Report 1958). Thus this event may also have involved rupture of an asperity at the plate interface, extending into conditionally stable subducted sediments.

## ACKNOWLEDGEMENTS

Valuable assistance with the fieldwork was provided by Mark Chadwick, and Russell Robinson helped with the earthquake relocations and focal mechanism determinations. We would like to dedicate this work to Professor Jim Ansell, who died shortly after being involved in the fieldwork. His enthusiasm for subduction studies was an inspiration to us all. The study was supported by the New Zealand Foundation for Research, Science and Technology. Institute of Geological and Nuclear Sciences contribution no. 1089.

## REFERENCES

1. Ansell, J.H. and Bannister, S.C., (1996). Shallow morphology of the subducted Pacific plate along the Hikurangi margin, New Zealand. *Phys. Earth Planet. Inters.*, **93**: 3-20.

2. Bannister, S., (1988). Microseismicity and velocity structure in the Hawkes Bay region, New Zealand: fine structure of the subducting Pacific plate. *Geophys. J.*, **95**: 45-62.

3. Chadwick, M., (1997). *The 1991 Hikurangi Margin seismic refraction experiment,* PhD thesis, Victoria University of Wellington, New Zealand.

4. Chong, F.K.L., (1982). *A microearthquake study of the Indian/Pacific plate boundary, central Hawkes Bay, New Zealand.* PhD thesis, Victoria University of Wellington, New Zealand.

5. Collot, J-Y. and 15 others, (1996). From oblique subduction to intra-continental transpression: structures of the southern Kermadec-Hikurangi Margin from multibeam bathymetry, side-scan sonar and seismic reflection, *Marine Geophys. Res.*, **18**, 357-381.

6. Cousins, W.J., Porritt, T.E., Hefford. R.T., Baguley, D.E., O'Kane, S.M. and McVerry, G.H., (1994). Computer analyses of New Zealand earthquake accelerograms 8: the Tikokino, Fiordland, and Ormond earthquakes of 1993. *Institute of Geological and Nuclear Sciences Science Report* **94/34**, 316 p.

7. DeMets, C., Gordon, R.G., Argus, D.F. and Stein, S., (1994). Effect of recent revisions to the geomagnetic reversal time scale on estimates of current plate motions. *Geophys. Res. Letts.*, **21**: 2191-2194.

8. Haines, A.J. and Darby, D.J., (1987). Preliminary dislocation models for the 1931 Napier and 1932 Wairoa earthquakes. New Zealand *Geological Survey report* EDS 114.

9. Ihmlé, P.F., (1996). Frequency-dependent relocation of the 1992 Nicaragua slow earthquake: an empirical Green's function approach. *Geophys. J. Int.*, **127**: 75-85.